

Dicamba Degradation by Fenton-Like Process Using Iron/Biochar Composites

Tiago Guimarães,^a Adalin C. M. de Aguiar,^b Elisa M. G. da Silva,^b Kamila C. Mielke,^b Marcelo M. da Costa,^c Antonio A. da Silva,^b Ana P. C. Teixeira^d and Renata P. Lopes^{b,*a}^aLaboratório de Química Analítica, Departamento de Química, Universidade Federal de Viçosa, Campus de Viçosa, 36570-000 Viçosa-MG, Brazil^bLaboratório de Manejo Integrado de Plantas Daninhas, Departamento de Fitotecnia, Universidade Federal de Viçosa, Campus de Viçosa, 36570-000 Viçosa-MG, Brazil^cLaboratório de Celulose e Papel, Departamento de Engenharia Florestal, Universidade Federal de Viçosa, Campus de Viçosa, 36570-000 Viçosa-MG, Brazil^dLaboratório de Química Inorgânica, Departamento de Química, Universidade Federal de Belo Horizonte, Campus de Belo Horizonte, 31270-901 Belo Horizonte-MG, Brazil

In this work, an iron/biochar composite was evaluated as a catalyst for 3,6-dichloro-2-methoxybenzoic acid (dicamba) herbicide degradation by heterogeneous Fenton-like process. The biochar was produced from pyrolysis of coffee husks. After Fe^{II} adsorption by biochar, the material was submitted to chemical reduction, via borohydride, producing zero-valent iron nanoparticles (BIO-Fe⁰). The material was characterized by Fourier transform infrared spectroscopy (FTIR), scanning electron microscopy and energy dispersive X-ray spectroscopy, Raman scattering spectroscopy, nitrogen adsorption/desorption analysis, among other techniques. The BIO-Fe⁰ is a heterogeneous material, and the main constituent elements are carbon (C), oxygen (O), silicon (Si), sulfur (S) and iron (Fe). The dicamba degradation was monitored by high-performance liquid chromatography and biological assays using beans (*Phaseolus vulgaris*) as indicator species. The commercial dicamba (500 mL; 250 mg L⁻¹) was submitted to Fenton-like process (initial pH 3.20; BIO-Fe⁰: 3 or 5 g; 1.00 mL H₂O₂ at 3.00 mmol L⁻¹; 1.00 mL Al₂(SO₄)₃ at 1.00 mol L⁻¹; 25 °C and 5 h of reaction), presenting ca. 100% of degradation. These treated solutions were used in a biological assay. The intoxication levels were less 30%. These results show that BIO-Fe⁰ has the potential to be used in the dicamba degradation by Fenton-like processes.

Keywords: biomass, advanced oxidative processes, biological assay (*Phaseolus vulgaris*), herbicides, residual water, adsorption/degradation

Introduction

The dicamba, 3,6-dichloro-2-methoxybenzoic acid, is a chlorobenzoic herbicide, widely used worldwide to weeds control in grain crops, pastures and non-crop areas.¹ This significant application is due to its high efficiency and low cost. Recently, it was developed genetically modified (GM) soybeans and cotton resistant to dicamba. Since these GM crops are planted on a large scale, the use of dicamba is expected to increase significantly.² The dicamba (C₈H₆Cl₂O₃) (Figure 1) has a molar mass of 221.04 g mol⁻¹ and pK_a 1.87, being of great environmental concern due to

its high-water solubility.³ Therefore, the development of new processes that guarantee its complete degradation are required, in order to minimize the environmental impacts caused by its inappropriate use and disposal.⁴

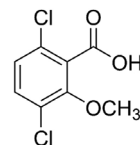


Figure 1. Molecular structure of dicamba.

During the application, the mixture containing pesticides must be properly calculated to avoid large surpluses at the end of the process. The residual liquid in the sprayer tank must be diluted in water and applied at the

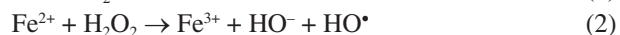
*e-mail: renataplopes@ufv.br

Editor handled this article: Maria Cristina Canela (Associate)

borders of the treated areas or on the pathways.⁵ However, for herbicide case, the spread it over treated areas can cause serious environmental problems. Dicamba is highly toxic to sensitive broad-leafed crops such as soybeans, for example.⁶ The use of herbicide doses beyond those recommended may be associated with the appearance of resistant weeds. Therefore, the development of dicamba degradation processes directly in the spray tank can be an important tool to avoid such problems.

The processes that govern the destination of most organic contaminants within the soil matrix include adsorption-desorption, chemical and biological degradation, volatilization, and transport.⁷ The infiltration of halogenated compounds into groundwater has generated considerable interest in recent years, since many of these contaminants can be degraded by dechlorination reactions.² In this sense, a technology that has been highlighted is the use of zero-valent metals to remediate surface and groundwater contaminated with different organic compounds.⁸ However, a disadvantage of the use of these materials in aqueous systems consists in the leaching of the metals. Thus, the use of biochar as a support can prevent this leaching problem,⁹ besides allowing a better dispersion of iron nanoparticles and reuse of these materials. Furthermore, zero-valent metals can be used in the advanced oxidative processes, such as Fenton reaction,¹⁰ and the sulfate radical-based processes (SO₄^{•-}).¹¹

Fenton processes (equation 1) are characterized by the hydroxyl radicals (HO[•]) production from the reaction of iron(II) catalyst and hydrogen peroxide. Such processes are very efficient in the degradation of different contaminants such as pharmaceuticals compounds¹² and herbicides.¹³ Fenton-like processes, on the other hand, consist of the HO[•] generation by other iron species (Fe⁰ or Fe³⁺),¹⁴ or even another metal, such as copper¹⁵ and zinc,¹⁶ for example. Among the main advantages of the Fenton process (equations 1-2) is its high efficiency of degradation,¹⁷ which can be further enhanced by incorporating radiation (ultraviolet or visible).¹⁸



Fenton-like processes are capable of oxidizing and mineralizing a large number of organic molecules, producing mostly CO₂ and inorganic ions.¹⁰ The mechanism of hydrocarbon oxidation catalyzed by hydroxyl radicals are described in equations 3-6.¹⁹ As can be seen, the oxidation of organic compounds (OC) is initiated by the hydroxyl radical (HO[•]), forming R[•] radicals, which are highly reactive and can also be oxidized.²⁰



A major challenge in the herbicide application consists in the proper disposal of residual water after the spray tank washing process. Thus, the objective of this study was to evaluate the dicamba degradation (commercial product) by iron nanoparticles supported on biochar derived from coffee husks (BIO-Fe⁰) via Fenton-like process, aiming to develop a technology capable of degrading the herbicide residue from spray tank.

Experimental

Standards and reagents

Sodium borohydride (98%) (CAS 16940-66-2) was purchased from Sigma-Aldrich (St. Louis, USA). Ferrous sulfate heptahydrate (98.9%) (CAS 7782-63-0), sodium hydroxide (NaOH) (95%) (CAS 1310-73-2), hydrochloric acid (HCl) (37%) (CAS 7647-01-10), hydrogen peroxide (H₂O₂) (33%) (CAS 7722-84-1), and aluminum sulfate (Al₂(SO₄)₃·16H₂O) (99.9%) (CAS10043-01-3) were purchased from Vetec (Rio de Janeiro, Brazil). All chemicals were used without further purification and were of analytical grade. All solutions were prepared with purified water type 1 (18.2 MΩ cm at 25 °C), which was obtained by Milli-Q[®] system (Millipore, Bedford, MA, USA).

Iron particles supported on biochar (BIO-Fe⁰)

The biochar used as a support for iron particles was produced from coffee husks (*Coffea arabica*) whose methodology and characterization results were described in a previous work.²¹ In general, the coffee husks was pyrolyzed under inert atmosphere at 350 °C, with a ramp of 10 °C min⁻¹, and a residence time of 3 h. This biochar (BIO350) was characterized and used as Fe^{II} adsorbent.

The zero valent-iron nanoparticles (nZVI) were incorporated into biochar (BIO350) according to the methodology adapted from Shi *et al.*,²² for the BIO-Fe⁰ production. Initially, 50.00 mL of ethanol:water (4:1, v/v) was added to 10.00 g of biochar with adsorbed Fe^{II} and the system was stirred for 30 min on a shaking table at 3000 rpm. Then, 100.00 mL of sodium borohydride solution (1.08 mol L⁻¹) was added to the system at 0.10 mL s⁻¹ under constant stirring. The system containing the solid material (BIO-Fe⁰) was vacuum filtered and then subjected to four washing steps, the first with 50.00 mL of Milli-Q[®] water

and the others with 50.00 mL of ethanol each. The BIO-Fe⁰ was dried in a rotary evaporator for 3 h and stored under refrigeration at -20 °C.

BIO-Fe⁰ characterization

The functional groups of BIO-Fe⁰ were analyzed by infrared spectroscopy (FTIR) in a Bruker VERTEX 70 instrument using the attenuated total reflectance (ATR) (Palo Alto, USA) method in the range 350-4000 cm⁻¹. X-ray diffraction (XRD) was performed on a D8-Discover diffraction system (Billerica, USA). The crystalline phase was compared with standard JCPDS files.

The surface morphology and elemental analysis of BIO-Fe⁰ were performed on a scanning electron microscope (JEOL brand, model JSM-6010LA) (Kyoto, Japan). This microscope has a resolution of 4 nm (with beam at 20 kV), magnification of 8× to 300.000×, and accelerating voltage of 500 V at 20 kV. It was used electron gun with pre-centered tungsten filament. Everhart-Thornley detector for secondary electron imaging and solid-state detector for backscattered electrons with variable topography, composition, and shading contrast silicon drift detector for energy-dispersive X-ray (EDS) analysis with 133 eV resolution.

Raman spectroscopy was performed on a micro-Raman spectrometer (Renishaw InVia) (Kansai, Japan) equipped with a Nd-YAG Ia ($\lambda_0 = 514$ nm) and a 50× objective lens (Olympus B x 41), and the Raman spectrum acquisition time for each sample was set as 10 s. The surface area and porous structure of BIO-Fe⁰ were determined by N₂ adsorption isotherms using Quantachrome Instruments, model Nova 1200e (Kyoto, Japan).

Dicamba degradation process

The dicamba degradation processes were carried out in three different steps, under constant agitation, and room temperature (25 °C).

(i) In the first step, 100.00 mL of dicamba standard solution and commercial product (25 mg L⁻¹, initial pH 3.20, and BIO350/BIO-Fe⁰ = 1.00 g) were used.

(ii) In the second step, 100.00 mL of the commercial product (25 or 250 mg L⁻¹, initial pH 3.20 and BIO-Fe⁰ = 1.00 g); 1.00 mL of H₂O₂ (1.00 mmol L⁻¹); 1.00 mL of Al₂(SO₄)₃ (1.00 mol L⁻¹) were used.

(iii) In the third step, the commercial product (500 mL at 250 mg L⁻¹ and initial pH 3.20) was used, and besides the composite (BIO-Fe⁰), 1.00 mL H₂O₂ (3.00 mmol L⁻¹); 1.00 mL Al₂(SO₄)₃ (1.00 mol L⁻¹) were added to the system, for two amounts of BIO-Fe⁰, 3.00 g (BIO-Fe⁰3g) and 5.00 g (BIO-Fe⁰5g).

The pH adjustment of the system to 3.20 was carried out using solutions of HCl or NaOH (both at 0.10 mol L⁻¹). The flasks were sealed with parafilm and shaken on an orbital shaker at 25 ± 2 °C. The pH of the solution was monitored during the reaction. After 24 h of reaction, a 2.00 mL aliquot was filtered on cellulose acetate membrane (0.45 µm pore size and 13 mm diameter Analytical) and analyzed by high-performance liquid chromatography (HPLC). The assays were performed in triplicate.

The HPLC system used was a Shimadzu model SCL-10A VP system controller (Kyoto, Japan), equipped with LC-10AD VP pump, SPD-10A VP UV detector, SCL-10A VP control center, and Rheodyne injector (injection volume 30 µL). HPLC operating conditions were: C18 column, Keystone NA (Keystone Scientific, Bellefonte, PA); oven temperature 35 °C, mobile phase of acetonitrile: H₂O (3:7 v/v) with 0.01% CH₃COOH in isocratic mode; flow rate of 1.00 mL min⁻¹, and quantification at 275 nm using a photodiode array detector.

Evaluation of the species responsible for dicamba degradation

To evaluate the species responsible for dicamba degradation, assays were performed using 100.00 mL of commercial dicamba solution (50.00 mg L⁻¹), 1.00 mL of hydrogen peroxide (1.00 mmol L⁻¹), 1.00 mL Al₂(SO₄)₃ 1.00 mol L⁻¹ and 0.50 g of BIO-Fe⁰, under constant agitation (3000 rpm), and room temperature (25 °C).

The inhibitors used were *tert*-butyl alcohol (TBA, 10.00 mmol L⁻¹), *p*-benzoquinone (*p*-BZQ, 10.00 mmol L⁻¹) or furfuryl alcohol (FFA, 10.00 mmol L⁻¹), to capture hydroxyl radicals (•OH), superoxide radicals (•O₂⁻) and singlet oxygen (¹O₂), respectively. The inhibitor solutions were prepared at the time of the assay. Thus, 1.00 mL of each inhibitor solution (10.00 mmol L⁻¹) was added to the dicamba solution just before the start of the reaction.

Biological assay

In the biological assay with bean indicator species (*Phaseolus vulgaris*), three seeds were sown in plastic pots of 0.33 dm³ filled with yellow Latosol. After plant emergence, the plants were thinned, leaving two plants *per* pot. When the bean plants reached the physiological stage V3, 500.00 mL of (i) commercial dicamba at 250 mg L⁻¹; (ii) solutions degraded by the Fenton-like process, according to the procedure described previously, whose initial concentration of the commercial dicamba was 250 mg L⁻¹; the material doses were 6.0 and 10.0 g L⁻¹ (BIO-Fe⁰); (iii) potable water (control) was applied in

different pots. The application was made with the aid of a CO₂ pressurized sprayer, equipped with two TT 11002 nozzles, spaced at 0.50 m, maintained at a pressure of 25 lb pol⁻² and a spray volume of 200 L ha⁻¹. At 7 and 14 days after application (DAA), intoxication scores were assigned to the bean plants, being zero for absence of symptoms and 100 for plant death.

Results and Discussion

The BIO-Fe⁰ characterization provides information about the chemical composition of the material, being quite useful in the understanding of the process that occur in the degradation processes. The FTIR results obtained are shown in Figure 2a. It is possible to observe the main functional groups present on the surface of BIO-Fe⁰. The band at 1036 cm⁻¹ can be attribute to C–O stretching of acids, esters, alcohol and ethers.²³⁻²⁵ The band at 1348 cm⁻¹ can be attributed to C=C stretching.^{21,26,27} The band at 1632 cm⁻¹ can be attributed to C–O stretching of acids and esters.²⁸ These bands are common in carbonaceous materials from biomass carbonization.²⁹

The diffractogram obtained for BIO-Fe⁰, Figure 2b, indicated an amorphous carbon structure ($2\theta = 15-35^\circ$)^{27,29} with a peak referring to crystallized silica ($2\theta = 30^\circ$).³⁰ These results are similar with reports described in the literature that used biochar as a support and/or as an environmental remediator. Liu *et al.*³¹ used biochar derived from peanut shells for doxycycline hydrochloride adsorption and the X-ray characterization showed an extended peak at $2\theta = 15-35^\circ$. Yin *et al.*³² also observed a peak at $2\theta = 30^\circ$ that was attributed to crystallized silica. According to authors, the biochar was produced from poplar bark and used for adsorption nitrate and phosphates. The presence of iron could not be observed by FTIR and XRD (Figures 2a-2b). According to Chen *et al.*,³³ this result can be attributed to the low concentration of iron in the sample (ca. 5%).

By Raman spectroscopy (Figure S1, Supplementary Information (SI) section) it is possible to observe the D band in 1359 cm⁻¹, referred to amorphous carbon, and G band in 1580 cm⁻¹, attributed to graphitic carbon structures.²⁵ The D and G bands are assigned to vibrational modes involving sp² bonded carbon. The D and G bands intensity ratio, that is, I_D/I_G, indicates the structural disorder degree of graphitic materials. BIO-Fe⁰ presented I_D/I_G = 0.93, typical for materials with some disorder degree.³⁴ Similar results were found by Zhou *et al.*,³⁵ who found I_D/I_G = 0.92 for biochar from bone. According to the authors, the material could carry defective edges containing oxygen or hydrogen on the surface.

The N₂ adsorption/desorption isotherm was performed for BIO-Fe⁰, and the result is shown in Figure S2 (SI section). As shown in Figure S2, the mesopore size distribution is predominantly in the 1-5 nm range. According to the International Union of Pure and Applied Chemistry (IUPAC) classification, the BIO-Fe⁰ material exhibits an intermediate isotherm of type I and II, associated with a combination of microporous-mesoporous structures.³⁶ The specific surface area of the BIO-Fe⁰ is approximately 1.50 m² g⁻¹. Irfan *et al.*³⁷ found specific surface areas of 2.10, 7.03 and 5.21 m² g⁻¹ for biomass from halophyte (*Achnatherum splendens* L.), biochar produced at 300 and 700 °C, respectively, showing that pyrolysis temperature also influences the material characteristics.

The BIO-Fe⁰ SEM image is shown in Figure 3a, and a porous material can be observed. Similar results are described in the literature.^{38,39} By EDS, Figure 3b, it is possible to observe that the main elements present in BIO-Fe⁰ are carbon (C), oxygen (O), silicon (Si), sulfur (S) and iron (Fe). The iron particles presented 10% m/m of the BIO-Fe⁰. The presence of silicon can be attributed to coffee husks composition.²¹

The BIO-Fe⁰ produced was used as catalyst in the dicamba degradation assays by Fenton-like process. The

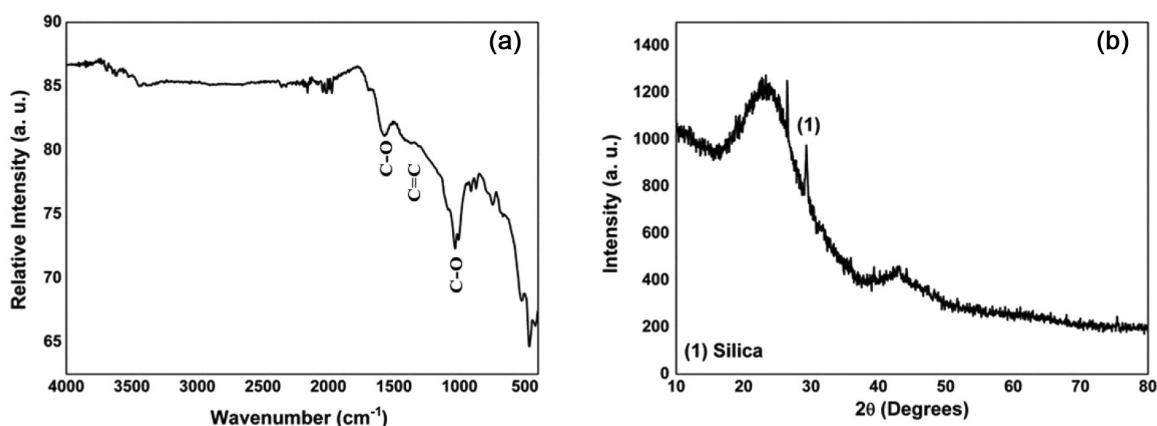


Figure 2. (a) FTIR (ATR) spectrum and (b) X-ray diffractogram for BIO-Fe⁰.

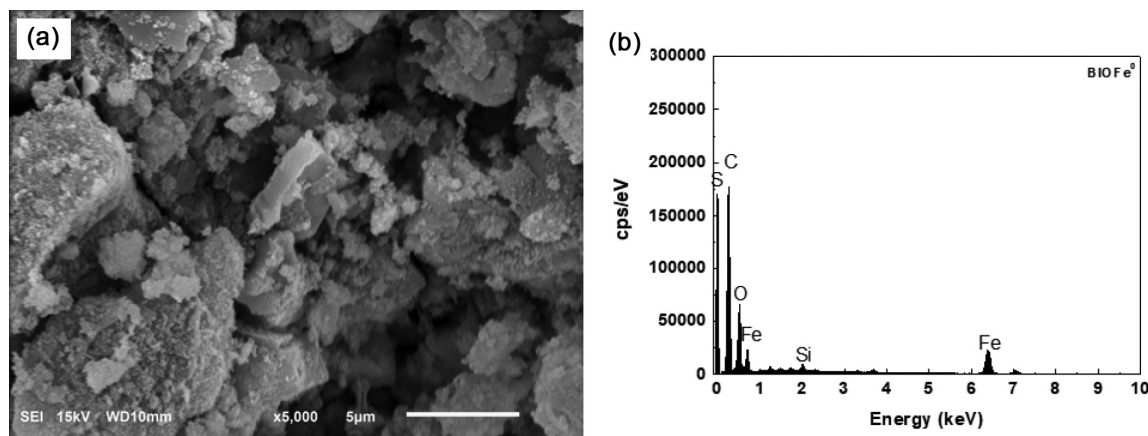


Figure 3. (a) Scanning electron microscopy image (resolution of 4 nm, with beam at 20 kV, magnification of 8× to 300.000×, and accelerating voltage of 500 V at 20 kV) and (b) chemical mapping (detector for EDS analysis with 133 eV resolution) of BIO-Fe⁰.

BIO-Fe⁰ can be used as heterogeneous catalyst,^{40,41} allowing its reuse⁴² and avoiding the leaching of iron to solution.⁴³ First, the chromatographic conditions were selected. The chromatogram of the dicamba standard solution is shown in Figure S3 (SI section). The dicamba presented a retention time of 11 min. After, control assays were performed using biochar from coffee husks (BIO350) and the iron particle/biochar composite (BIO-Fe⁰) to treat the dicamba standard solution (Figure 4a), and the commercial product solution (Figure 4b). As can be seen in Figure 4a, the dicamba degradation is not significant for both materials, only ca. 8%. The use of Fe⁰ for dicamba degradation has been reported by Maya-Treviño *et al.*⁴⁴ but, according to the authors, the reaction is very slow and with low degradation efficiency. As can be seen in Figure 4b, the removal efficiency remained low (ca. 9%) also for the commercial product. As the results were similar for the analytical standard and the commercial product, the following experiments were carried out with the commercial product, aiming to simulate a real field situation, and because the analytical standard is relatively more expensive than the commercial product.

Thus, in the second step, new assays were performed using the commercial product in the initial concentration of dicamba of 25 and 250 mg L⁻¹, in which hydrogen peroxide and aluminum salt were added to the reaction. As can be seen in Figure 5, the dicamba degradation by Fenton-like reaction in the presence of aluminum salt was effective. The degradation reached about 100% for both concentrations, i.e., 25 and 250 mg L⁻¹.

The hydroxyl radical is a strong non-selective oxidizing agent that reacts with organics, originating dehydrogenated or hydroxylated derivatives, until their mineralization. For example, Pignatello⁴⁵ reported the complete destruction of a 0.10 mM 2,4-dichlorophenoxyacetic acid solution at pH 3.00 through oxalic acid using H₂O₂/Fe²⁺ and H₂O₂/Fe³⁺/UV. According to Brillas *et al.*,¹ aluminum species may favor the reaction by contributing to the solution pH remain acidic (pH ≤ 3.00), and according to equation 7, preventing the iron precipitation.¹

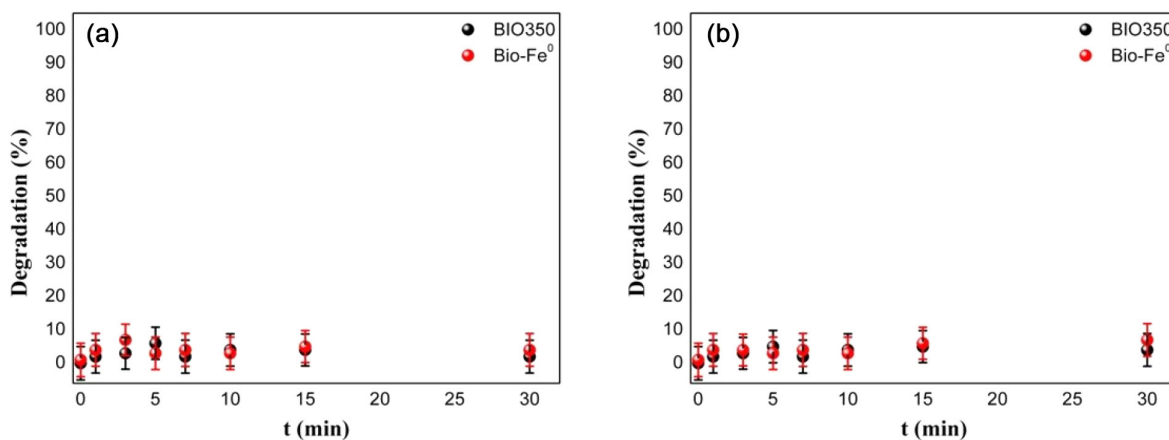


Figure 4. Removal of analytical standard (a) and commercial product (b) of dicamba by BIO350 and BIO-Fe⁰. Conditions: volume of solution: 100.00 mL; C_i = 25 mg L⁻¹; BIO350/BIO-Fe⁰ (Fe 10% m/m) = 1.00 g; pH = 3.20.

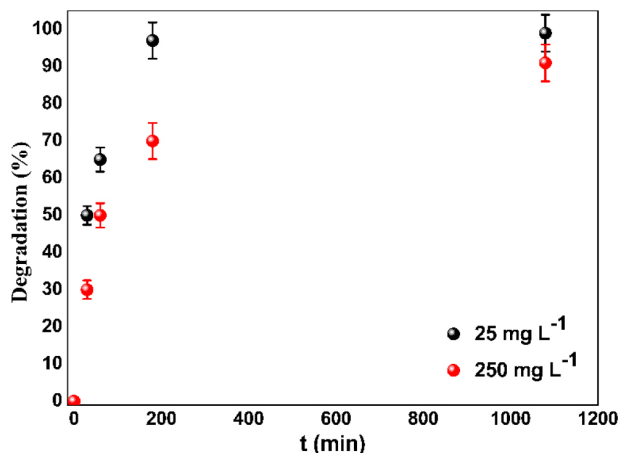


Figure 5. Removal of commercial dicamba (initial concentration: 25 or 250 mg L⁻¹). Experimental conditions: volume of solution = 100.00 mL; BIO-Fe⁰ = 1.00 g; 1.00 mL of H₂O₂ (1.00 mmol L⁻¹); 1.00 mL of Al₂(SO₄)₃ (1.00 mol L⁻¹).

Another point to be highlighted is the possible improvement in the efficiency of the reaction, acting on the dechlorination of dicamba and on the formation of hydroxyl radicals.⁴⁶

Aiming to approximate field conditions, in the third step, new studies were performed, employing 500.00 mL of commercial dicamba product (250 mg L⁻¹) and two doses of BIO-Fe⁰. The concentration of 250 mg L⁻¹ was chosen because it is a concentration close to that found in spray tanks, while the volume (500.00 mL) was selected due to the demand for a little more volume for application with the sprayer. The results are shown in Figure 6.

As can be seen in Figure 6, the degradation of the commercial product by the Fenton-like process by BIO-Fe⁰ was 85 ± 3% and 95 ± 3% for 3.00 and 5.00 g, respectively. This can be explained by the amount of catalyst (iron) present in the biochar, which is responsible for the formation of hydroxyl radicals, that is, the more iron available in the system, the greater the formation of radicals, causing the degradation of dicamba in a catalytic reaction in a cycle in which Fe^{II} is regenerated.⁴⁷

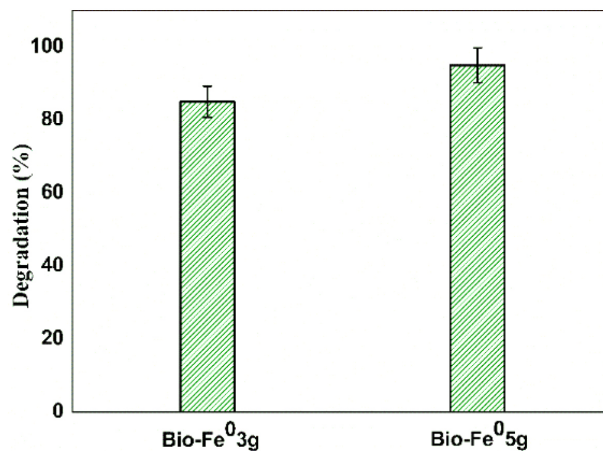


Figure 6. Removal of commercial dicamba. Experimental conditions: volume of solution = 500.00 mL; C_i = 250 mg L⁻¹; BIO-Fe⁰ = 3.00 and 5.00 g; 1.00 mL H₂O₂ (3.00 mmol L⁻¹); 1.00 mL Al₂(SO₄)₃ (1.00 mol L⁻¹); 25 °C and 5 h of reaction.

After the degradation reactions, the solutions were applied to bean plants and the results for 7 and 14 days after application (DAA) are presented in Figures 7 and S4 (SI section), respectively.

The choice of beans (*Phaseolus vulgaris*) as a bioindicator plant is due to this species being sensitive to the presence of dicamba in solution. The presence of herbicides in soil and water can be carried out by bioassays using sensitive indicator species. These plants must be easy to grow, have rapid development and sensitive to the evaluated herbicide.⁴⁸ Commercial dicamba interferes in the action of the ribonucleic acid (RNA)-polymerase enzyme and, consequently, in the synthesis of nucleic acids and proteins. This herbicide induces intense cell proliferation. As a result, there is a disorganized growth of the tissues, which leads the plant to suffer epinasty of the leaves, twisting of the stem, thickening of the terminal buds and death of the plant.

These symptoms were more pronounced when the commercial product (at 250 mg L⁻¹ of dicamba) was applied to the bean plants. In contrast, when the commercial product was treated with 5.00 g (Figure 7b) and 3.00 g (Figure 7c) of BIO-Fe⁰ in a Fenton-like process,

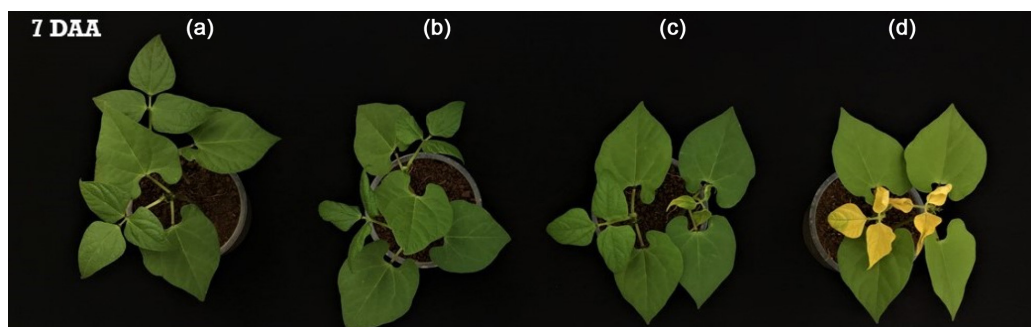


Figure 7. Injury levels in beans of dicamba degradation products by Fenton-like processes at 7 days after application (DAA) (a) control, (b) 95% degradation (BIO-Fe⁰5g) (c), 85% degradation (BIO-Fe⁰3g) (d) and commercial dicamba 250 mg L⁻¹.

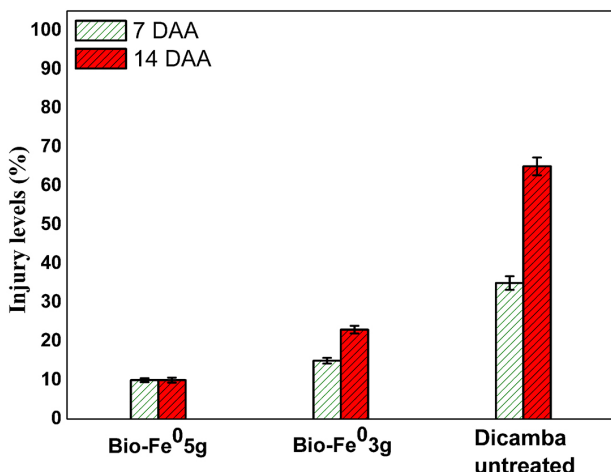


Figure 8. Intoxication of dicamba degradation products by Fenton-like processes employing beans as indicator species at 7 and 14 DAA (days after application).

the injuries were less pronounced. Injury level scores were assigned to the bean plants and the results are presented in Figure 8.

Dicamba is a toxic product to sensitive plants, in which even at very low concentrations present visible signs of intoxication, due to the compromised development of these plants. When the solution was treated by a Fenton-like process, using 5.00 g of BIO-Fe⁰, the symptoms did not reach 10%, damage from which a plant would probably be able to recover. In contrast, the application of dicamba without treatment (250 mg L⁻¹) exceeded 60% of intoxication of the plants, damage that would lead to the death of the plant.

In order to better understand the degradation pathway of dicamba by BIO-Fe⁰, assays using radical inhibitors were performed and the results are shown in Figure 9. To evaluate the contribution of different reactive oxygen

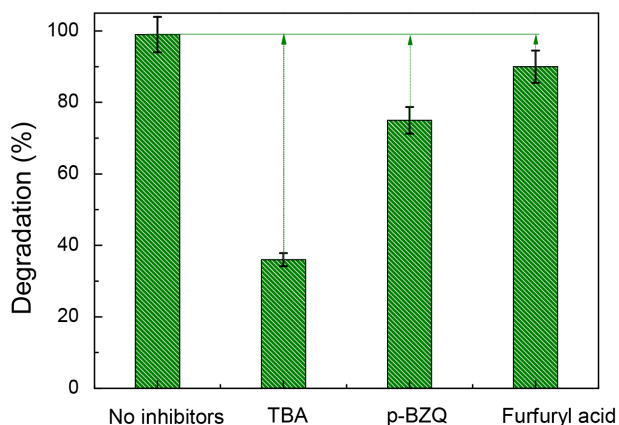


Figure 9. Effect of different chemical inhibitors on the dicamba degradation. Experimental conditions; volume of solution: 100.00 mL; C_i = 50 mg L⁻¹; BIO-Fe⁰ = 0.50 g; 1.00 mL of H₂O₂ (1.00 mmol L⁻¹); 1.00 mL of Al₂(SO₄)₃ (1.00 mol L⁻¹); 1.00 mL of each of the inhibitors at 10.00 mmol L⁻¹. TBA is *tert*-butyl alcohol and *p*-BZQ is *p*-benzoquinone.

species, *tert*-butyl alcohol, *p*-benzoquinone (*p*-BZQ) and furfuryl alcohol (FFA) were chosen as chemical inhibitors of •OH, •O₂⁻ and ¹O₂, respectively.⁴⁹

Furfuryl alcohol, responsible for inhibiting ¹O₂ radicals, inhibited 9% of dicamba degradation in 300 min of reaction. On the other hand, *p*-BZQ inhibits almost 25% of dicamba, indicating that •O₂⁻ plays an important role in this degradation system, as reported by other authors.⁴⁹ The suppressant that showed the highest inhibition effect, however, is *tert*-butyl alcohol, preventing 65% degradation in 300 min, indicating that the •OH radical plays the most important role among the species responsible for dicamba degradation, corroborating with results already revealed in the literature, for similar systems.⁵⁰

Conclusions

The iron/biochar composite (BIO-Fe⁰) derived from coffee husks was successfully synthesized and applied in the degradation of dicamba in aqueous systems by heterogeneous Fenton-like process. The process simulated spray tank wastewater, with a high concentration of dicamba. The BIO-Fe⁰ synthesis can be considered sustainable, as it uses biomass residues as the starting material. The adsorption process was little significant, corresponding to 8% of removal. On the other hand, the degradation by heterogeneous Fenton-like process was quite pronounced (approximately 100%), confirmed by the chromatographic analyzes. The main mechanism involves the OH radicals, using the iron particles present on the surface of the Bio-Fe⁰. The treated dicamba solution was submitted to biological assay using beans as indicator species showing toxicity levels lower than 30%. Thus, the BIO-Fe⁰ composite has the potential to be deployed in a spray tank dicamba residue degradation technology, being a viable, low-cost and environmentally safe alternative.

Supplementary Information

Supplementary information (Raman spectra, N₂ adsorption/desorption isotherms, pore distribution of BIO-Fe⁰ and injury levels in beans of dicamba degradation products by Fenton-like processes at 14 days after application (DAA)) is available free of charge at <http://jbc.sbq.org.br> as PDF file.

Acknowledgments

We thank the Coordenação de Aperfeiçoamento de Pessoal de Nível Superior - Brazil (CAPES), Conselho Nacional de Desenvolvimento Científico e Tecnológico

(CNPq), Fundação de Amparo à Pesquisa do Estado de Minas Gerais (FAPEMIG) - process: APQ-01275-18, and INCT Midas; to the Laboratory of Nanomaterials and Environmental Chemistry (LaNaQuA-UFV), the Laboratory of Integrated Weed Management (MIPD-UFV) Laboratory of Cellulose and Paper (LCP-UFV) and the Microscopy Center of the Federal University of Minas Gerais.

Author Contributions

Tiago Guimarães was responsible for conceptualization, methodology, investigation, formal analysis, writing-original draft, review and editing; Adalin Cezar Moraes de Aguiar for investigation, formal analysis, writing original draft; Elisa Maria Gomes da Silva for investigation, formal analysis, writing original draft; Kamila Cabral Mielke for investigation, formal analysis, writing original draft; Marcelo Moreira da Costa for formal analysis, writing-review and editing, supervision; Antonio Alberto da Silva for formal analysis, writing-review and editing, supervision; Ana Paula de Carvalho Teixeira for conceptualization, methodology, resources, funding acquisition, investigation, formal analysis, writing review and editing, supervision; Renata Pereira Lopes for conceptualization, methodology, resources, funding acquisition, investigation, formal analysis, writing-review and editing, supervision.

References

- Brillas, E.; Baños, M. A.; Garrido, A.; *Electrochim. Acta* **2003**, *48*, 1697. [Crossref]
- Yao, L.; Jia, X.; Zhao, J.; Cao, Q.; Xie, X.; Yu, L.; He, J.; Tao, Q.; *Int. Biodeterior. Biodegrad.* **2015**, *104*, 324. [Crossref]
- Gibb, C.; Satapanajaru, T.; Comfort, S. D.; Shea, P. J.; *Chemosphere* **2004**, *54*, 841. [Crossref]
- Chu, W.; Wong, C. C.; *Water Res.* **2004**, *38*, 1037. [Crossref]
- Menten, J. O. M.; Canale, M. C.; Calaça, H. A.; Flôres, D.; *Citr. Res. Tech.* **2017**, *32*, 109. [Link] accessed in May 2023
- Silva, D. R. O.; Silva, E. D. N.; Aguiar, A. C. M.; Novello, B. D. P.; Silva, Á. A.; Basso, C. J.; *Cien. Rural* **2018**, *48*, e20180179. [Crossref]
- Pavel, E. W.; Lopez, A. R.; Berry, D. F.; Smith, E. P.; Reneau Jr., R. B.; Mostaghimi, S.; *Water Res.* **1999**, *33*, 87. [Crossref]
- Xiang, S.; Cheng, W.; Nie, X.; Ding, C.; Yi, F.; Asiri, A. M.; Marwani, H. M.; *J. Taiwan Inst. Chem. Eng.* **2018**, *85*, 186. [Crossref]
- Álvarez, M. L.; Gascó, G.; Palacios, T.; Paz-Ferreiro, J.; Méndez, A.; *J. Anal. Appl. Pyrolysis* **2010**, *151*, 104893. [Crossref]
- Shawaqfeh, A. T.; Al Momani, F. A.; *Sol. Energy* **2010**, *84*, 1157. [Crossref]
- Guo, T.; Jiang, L.; Wang, K.; Li, Y.; Huang, H.; Wu, X.; Zhang, G.; *Appl. Catal., B* **2021**, *286*, 119883. [Crossref]
- Wu, Y.; Yang, Y.; Liu, Y.; Zhang, L.; Feng, L.; *Chem. Eng. J.* **2019**, *358*, 1332. [Crossref]
- Gu, J.-G.; Fan, Y.; Gu, J.-D.; *Chemosphere* **2003**, *52*, 1515. [Crossref]
- Feng, Y.; Liu, P.; Wang, Y.; Finfrook, Y. Z.; Xie, X.; Su, C.; Xu, Y.; *J. Hazard Mater.* **2019**, *384*, 121342. [Crossref]
- de Sousa, P. V. F.; de Oliveira, A. F.; da Silva, A. A.; Lopes, R. P.; *Environ. Sci. Pollut. Res.* **2019**, *26*, 14883. [Crossref]
- Tamayao, P. J.; Ribeiro, G. O.; McAllister, T. A.; Yang, H. E.; Saleem, A. M.; Ominski, K. H.; McGeough, E. J.; *Anim. Feed Sci. Technol.* **2020**, *273*, 114802. [Crossref]
- Chu, J.-H.; Kang, J.-K.; Park, S.-J.; Lee, C.-G.; *J. Water Process Eng.* **2020**, *37*, 101455. [Crossref]
- Gholami, P.; Dinpazhoh, L.; Khataee, A.; Orooji, Y.; *Ultrason. Sonochem.* **2019**, *55*, 44. [Crossref]
- Gabet, A.; Métivier, H.; de Brauer, C.; Mailhot, G.; Brigante, M.; *J. Hazard. Mater.* **2021**, *405*, 124693. [Crossref]
- Kim, J. R.; Kan, E.; *J. Environ. Manage.* **2016**, *180*, 94. [Crossref]
- Guimarães, T.; Teixeira, A. P. C.; de Oliveira, A. F.; Lopes, R. P.; *New J. Chem.* **2020**, *44*, 3322. [Crossref]
- Shi, L.; Zhang, X.; Chen, Z.; *Water Res.* **2010**, *45*, 886. [Crossref]
- Reza, M. S.; Afroze, S.; Bakar, M. S.; Saidur, R.; Aslfattahi, N.; Taweekun, J.; Azad, A. K.; *Biochar* **2020**, *2*, 239. [Crossref]
- Guimarães, T.; Luciano, V. A.; Silva, M. S. V.; Teixeira, A. P. C.; da Costa, M. M.; Lopes, R. P.; *Environ. Nanotechnol., Monit. Manage.* **2021**, *17*, 100645. [Crossref]
- Lopes, R. P.; Astruc, D.; *Coord. Chem. Rev.* **2021**, *426*, 213585. [Crossref]
- Özçimen, D.; Ersoy-Meriçboyu, A.; *Renewable Energy* **2009**, *35*, 1319. [Crossref]
- Ribeiro, M. R.; Guimarães, Y. M.; Silva, I. F.; Almeida, C. A.; Silva, M. S. V.; Nascimento, M. A.; Lopes, R. P.; *J. Environ. Chem. Eng.* **2021**, *9*, 105367. [Crossref]
- Wang, Y.; Wang, L.; Fang, G.; Herath, H. M. S. K.; Wang, Y.; Cang, L.; Xie, Z.; Zhou, D.; *Environ. Pollut.* **2013**, *172*, 86. [Crossref]
- Meili, L.; Lins, P. V.; Zanta, C. L. P. S.; Soletti, J. I.; Ribeiro, L. M. O.; Dornelas, C. B.; Silva, T. L.; Vieira, M. G. A.; *Appl. Clay Sci.* **2013**, *168*, 11. [Crossref]
- Lopes, R. P.; Guimarães, T.; Astruc, D.; *J. Braz. Chem. Soc.* **2021**, *32*, 1680. [Crossref]
- Liu, S.; Xu, W. H.; Liu, Y. G.; Tan, X. F.; Zeng, G. M.; Li, X.; Cai, X.-X.; *Sci. Total Environ.* **2017**, *592*, 546. [Crossref]
- Yin, Q.; Ren, H.; Wang, R.; Zhao, Z.; *Sci. Total Environ.* **2018**, *631*, 903. [Crossref]
- Chen, J.; Qiu, J.; Wang, B.; Feng, H.; Ito, K.; Sakai, E.; *J. Electroanal. Chem.* **2017**, *804*, 232. [Crossref]
- Kim, D.-G.; Ko, S.-O.; *Chem. Eng. J.* **2020**, *399*, 125377. [Crossref]

35. Zhou, X.; Zeng, Z.; Zeng, G.; Lai, C.; Xiao, R.; Liu, S.; Huang, D.; Qin, L.; Liu, X.; Li, B.; Yi, H.; Fu, Y.; Li, L.; Wang, Z.; *Chem. Eng. J.* **2020**, *383*, 123091. [Crossref]
36. Thommes, M.; Kaneko, K.; Neimark, A. V.; Olivier, J. P.; Rodriguez-Reinoso, F.; Rouquerol, J.; Sing, K. S. W.; *Pure Appl. Chem.* **2015**, *87*, 1051. [Crossref]
37. Irfan, M.; Chen, Q.; Yue, Y.; Pang, R.; Lin, Q.; Zhao, X.; Chen, H.; *Bioresour. Technol.* **2016**, *211*, 457. [Crossref]
38. Qian, K.; Kumar, A.; Zhang, H.; Bellmer, D.; Huhnke, R.; *Renewable Sustainable Energy Rev.* **2015**, *42*, 1055. [Crossref]
39. Ghani, W. A. W. A. K.; Mohd, A.; da Silva, G.; Bachmann, R. T.; Taufiq-Yap, Y. H.; Rashid, U.; Al-Muhtaseb, A. H.; *Ind. Crops Prod.* **2013**, *44*, 18. [Crossref]
40. Shan, A.; Idrees, A.; Zaman, W. Q.; Abbas, Z.; Ali, M.; Rehman, M. S. U.; Hussain, S.; Danish, M.; Gu, X.; Lyu, S.; *J. Environ. Chem. Eng.* **2021**, *9*, 104808. [Crossref]
41. Zhang, T.; Zhou, T.; He, L.; Xu, D.; Bai, L.; *Synth. Met.* **2020**, *267*, 116479. [Crossref]
42. Matos, T. T. S.; Fornari, M. R.; Mangrich, A. S.; Schultz, J.; Batista, E. M. C. C.; Ribeiro, R. O. C.; Romaõ, L. P. C.; Yamamoto, C. I.; Grasel, F. S.; Bayer, C.; Dieckow, J.; Bittencourt, J. D. A.; *J. Environ. Chem. Eng.* **2021**, *9*, 105472. [Crossref]
43. Wu, X.; Li, T.; Wang, R.; Zhang, Y.; Liu, W.; Yuan, L.; *Sep. Purif. Technol.* **2021**, *279*, 119768. [Crossref]
44. Maya-Treviño, M. L.; Guzmán-Mar, J. L.; Hinojosa-Reyes, L.; Ramos-Delgado, N. A.; *Ceram. Int.* **2014**, *40*, 8701. [Crossref]
45. Pignatello, J. J.; *Environ. Sci. Technol.* **1992**, *26*, 944. [Crossref]
46. Das, S. K.; Ghosh, G. K.; Avasthe, R. K.; Sinha, K.; *J. Environ. Manage.* **2021**, *278*, 111501. [Crossref]
47. Xiang, W.; Ji, Q.; Xu, C.; Guo, Y.; Liu, Y.; Sun, D.; Zhou, W.; Xu, Z.; Qi, C.; Yang, S.; Li, S.; Sun, C.; He, H.; *Appl. Catal., B* **2021**, *285*, 119847. [Crossref]
48. da Silva, A. A.; Silva, J. F.; *Tópicos em Manejo de Plantas Daninhas*, vol. 1, 1st ed.; Viçosa: Viçosa, Brazil, 2007.
49. Bicalho, H. A.; Rios, R. D. F.; Binatti, I.; Ardisson, J. D.; Howarth, A. J.; Lago, R. M.; Teixeira, A. P. C.; *J. Hazard. Mater.* **2020**, *400*, 123310. [Crossref]
50. Ma, X.; Cheng, Y.; Ge, Y.; Wu, H.; Li, Q.; Gao, N.; Deng, J.; *Ultrason. Sonochem.* **2018**, *40*, 763. [Crossref]

Submitted: January 19, 2023

Published online: May 5, 2023

